Rare Metal Materials and Engineering
Volume 55, Issue 10, October 2026
Available online at www.rmme.ac.cn

Science Press

Cite this article as: Zhong Hao, Dong Xiongbo, Yang Wei, et al. Enhancing Microstructure and Mechanical Properties of As-Cast Mg-12Gd-0.5Zr Alloys via Ultrasonic Treatment[J]. Rare Metal Materials and Engineering, 2026, 55(10): 2476-2483. DOI: https://doi.org/10.12442/j.issn.1002-185X.20250556.

ARTICLE

Enhancing Microstructure and Mechanical Properties of As-Cast Mg-12Gd-0.5Zr Alloys via Ultrasonic Treatment

Zhong Hao[1,3], Dong Xiongbo[2], Yang Wei[1], Wang Xueyi[2], Ma Zhijun[1], Yang Zhong[1]

[1] School of Materials Science and Chemical Engineering, Xi'an Technological University, Xi'an 710021, China; [2] Shaanxi Railway Institute, Weinan 714000, China; [3] Yulin University, Yulin 719000, China

Abstract: The influence of ultrasonic treatment on the microstructure and tensile properties of as-cast Mg-12Gd-0.5Zr alloys was examined. The results indicate that ultrasonic treatment markedly refines the α-Mg grain structure, with the finest grains observed at an input power of 1500 W. This grain refinement is attributed to the combined effects of cavitation and acoustic streaming, which promote heterogeneous nucleation. Furthermore, the treatment reduces the size and number of the secondary Mg_5Gd phase while enhancing its spatial uniformity. A considerable dissolution of Gd atoms into the α-Mg matrix is also observed, likely due to the suppression of Gd segregation by acoustic streaming. Correspondingly, ultrasonic treatment yields notable improvements in ultimate tensile strength, yield strength, and elongation at room temperature. These improvements are primarily attributed to the refined microstructure and the increased solid solubility of Gd within the matrix.

Key words: Mg alloy; ultrasonic treatment; grain refinement; tensile properties

1 Introduction

Magnesium (Mg) alloys have attracted significant interest in recent years due to their low density, high specific strength, and excellent machinability, making them promising materials for applications in the automotive, aerospace, and electronics sectors[1–4]. Among various alloying additions, rare-earth elements such as gadolinium (Gd) have been shown to markedly improve the mechanical properties and thermal stability of Mg alloys[5–7]. In particular, Mg-Gd alloys exhibit enhanced strength and creep resistance, which are highly advantageous for demanding structural applications[8–10].

However, the casting of Mg-Gd alloys frequently produces coarse-grained structures and a non-uniform distribution of secondary phases, which adversely affect their mechanical performance[11–13]. Therefore, effective grain refinement and control of phase distribution are essential for improving alloy performance[14]. Conventional grain-refinement techniques, such as alloying and thermal treatments, are often incapable to achieve the desired microstructural features[15–16].

Ultrasonic treatment has emerged as an effective non-contact approach for microstructural control in metallic systems, primarily by leveraging acoustic cavitation and streaming to accelerate nucleation and mitigate elemental segregation[17–19]. During treatment, cavitation-induced shockwaves fragment dendritic structures, while acoustic streaming facilitates solute homogenization, thereby collectively contributing to the refinement of as-cast microstructures[20]. Recent investigations have confirmed that the application of ultrasonic treatment to Cu-, Al-, Ti-, and Mg-based alloys significantly refines microstructures and improves compositional uniformity, thereby representing a nearly ideal strategy for achieving strength-ductility synergy[21–23]. Tong et al[24] examined the influence of ultrasonic treatment on the microstructure and mechanical properties of Mg-8Gd alloy, reporting a finer grain structure and substantially higher strength in ultrasonically treated samples compared with untreated counterparts. Additionally,

Received date: October 19, 2025
Foundation item: System and Technology of Bypass Coupled Arc MIG High Speed Welding (22019-86-84); Key Technologies and Applications for the Industrialization of High-Performance Aluminum Alloy Composites (2023-LL-QY—33); Aluminum-Magnesium Light Alloy Composite Materials Innovation Team of Shaanxi Railway Institute (KJTD202302)
Corresponding author: Ma Zhijun, Ph. D., Professor, School of Materials Science and Chemical Engineering, Xi'an Technological University, Xi'an 710021, P. R. China, Tel: 0086-29-86173324, E-mail: mazhijun@xatu.edu.cn

ultrasonic treatment improved the uniformity of melt temperature and Gd distribution, thereby reducing variation in mechanical properties along the melt height. Yang et al[25] demonstrated that ultrasonic treatment applied to Mg-Ni-Y alloy melt leads to significant refinement and uniform dispersion of secondary phases, particularly in long-period stacking ordered structures. Although the effectiveness of ultrasonic treatment in enhancing grain structure and mechanical behavior has been established across various alloy systems, its impact on Mg-Gd alloys remains underexplored, particularly regarding its ability to regulate the thermally stable Mg_5Gd phases and optimize Gd solute distribution, both of which are essential to aging response and elevated-temperature performance.

Mg-Gd series magnesium alloys, recognized for their lightweight nature, heat resistance, and exceptional mechanical properties at both room and elevated temperatures, have consistently been a focus of research worldwide. This study investigated the Mg-12Gd-0.5Zr alloy to elucidate the dual mechanism by which ultrasonic power influences its microstructural evolution. The optimal ultrasonic treatment parameters were determined through microstructural characterization and mechanical test, with particular emphasis on the effect of ultrasonication on secondary phases. This approach provides important insight for the development of high-performance Mg alloys via advanced processing methods.

2 Experiment

The Mg-12Gd-0.5Zr alloy was synthesized using pure Mg (99.9wt%), Mg-30wt% Gd (99.9wt%), and Mg-30wt% Zr master alloys. Melting was conducted at 760 ° C under a protective atmosphere of 0.1vol% SF_6 and 99.9vol% N_2, and the melt was held at this temperature to ensure complete dissolution of the master alloys. The degassed metal was first poured into a preheated metal mold (300 °C; dimensions: 380 mm×110 mm×165 mm), corresponding to the condition without ultrasonic treatment (0 W). Subsequently, the melt was ultrasonically treated at 720 °C for 90 s at power levels of 700, 1000, 1500, and 2000 W, and then cast into the same mold. The ultrasonic system (YPR59B-ZB, Hangzhou Success Ultrasound Equipment Co., Ltd, China) consisted of a 3 kW acoustic generator, an air-cooled piezoelectric transducer operating at 20 kHz, three horns, and a titanium alloy (Ti-6Al-4V) acoustic radiator with a diameter of 30 mm. To prevent Ti contamination, the radiator was coated with a mold release layer composed of ZnO and sodium silicate. The ultrasound parameters were approximately 30 μm in amplitude and 20 kHz in frequency. To mitigate the chill effect, the sonotrode was preheated to 700 ℃ before immersion to a depth of 20 mm below the melt surface[26].

For microstructural characterization, samples were polished to a mirror-like finish with diamond abrasives and etched in a 0.5vol% aqueous HNO_3 solution for 30 s. The microstructural evolution was investigated using a scanning electron microscope (SEM), energy-dispersive X-ray spectroscope (EDS), and an optical microscope (OM). The chemical composition of intermetallic phases was determined by EDS, while the α -Mg grain size and the area fraction of intermetallic phases were quantitatively analyzed using Image-Pro Plus 6.0 software.

Tensile test was conducted at room temperature on an Instron 4206 testing machine at a crosshead speed of 1.5 mm/min. For each alloy and testing condition, three dog-bone-shaped tensile specimens (gauge section: Φ6 mm×60 mm) were tested.

3 Results and Discussion

3.1 Thermodynamic calculation

Fig. 1 illustrates JMatPro thermodynamic simulations of the microstructural evolution of the Mg-12Gd-0.5Zr alloy under the Scheil-Gulliver solidification conditions. In Fig. 1a, the temperature-dependent variation in the equilibrium phase mass fraction is shown. The simulation suggests that Mg, Gd, and Zr form α-Mg, α-Zr, and Mg_5Gd phases during solidification. Among these, the α-Mg and α-Zr phases precipitate during the initial solidification stage, whereas the Mg_5Gd phase forms via a complex eutectic reaction as solidification proceeds. Fig. 1b further confirms that α-Zr and α-Mg are the first to precipitate, followed by the eutectic formation of Mg_5Gd. Fig. 1c shows the evolution of the liquid-phase chemical composition as the temperature decreases. During the pre-eutectic stage, the Mg content in the liquid remains high (approximately 85%), promoting the primary precipitation of α-Mg and α-Zr phases. As the eutectic reaction proceeds, Mg is progressively depleted, leading to an increase in Gd concentration in the liquid phase, which, in turn, promotes the formation of the Mg_5Gd phase.

3.2 Microstructure characterization

Fig. 2 presents OM images of the Mg-12Gd-0.5Zr alloy at various ultrasonic power levels. In all as-cast conditions, the alloys exhibit a white α-Mg matrix phase and intermetallic compounds at the grain boundaries. These intermetallics form interconnected morphologies, appearing as continuous or discontinuous network-like structures. In the absence of ultrasonic treatment, the α-Mg grains display coarse dendritic morphologies. Upon the sequential application of ultrasonic powers of 700, 1000, 1500, and 2000 W, the dendritic structures are progressively broken up, and the grains become increasingly rounded. This transformation indicates that ultrasonic treatment promotes a transition from dendritic to fully equiaxed grain growth. Fig. 2f summarizes the α-Mg grain sizes under different ultrasonic powers. As shown, the grain size initially decreases and subsequently increases with increasing ultrasonic power, reaching a minimum of 31.4± 1.8 μm at 1500 W. The corresponding measured grain sizes at 0, 700, 1000, 1500, and 2000 W are 51.6±2, 45.2±1.5, 40.6±1, 31.4±1.8, and 33.5±1.2 μm, respectively. These results confirm that ultrasonic treatment significantly refines the microstructure of the Mg-12Gd-0.5Zr alloy.

Following ultrasonic treatment, the α-Mg grain size in the

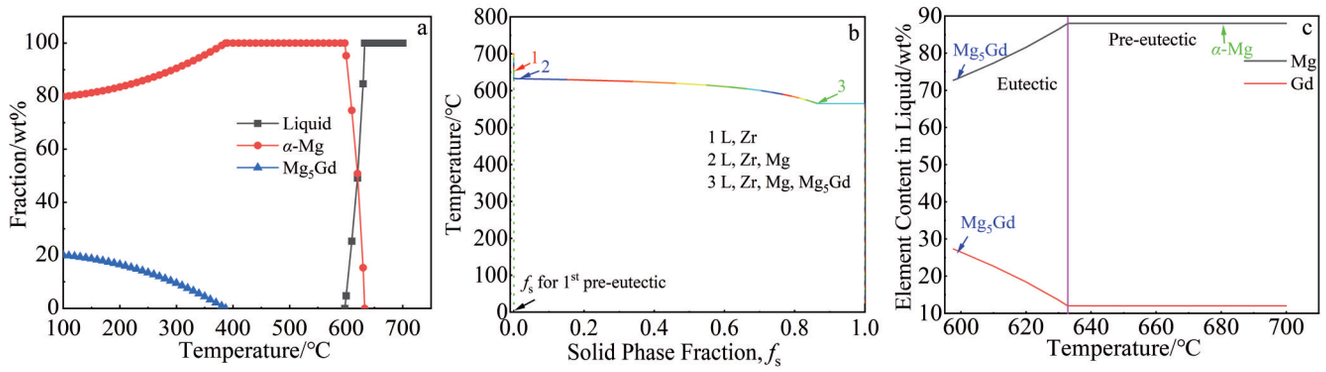

Fig.1 Fraction of equilibrium phases in Mg-12Gd-0.5Zr alloy (a); variation of solid phase fraction with temperature during solidification (b); variation in liquid-phase chemical composition with temperature (c)

alloy is markedly refined, primarily due to cavitation and acoustic streaming effects induced by ultrasound. During sonication, numerous microscopic cavitation bubbles are generated at the tip of the ultrasonic horn and propagate throughout the melt[23]. The nucleation and subsequent expansion of these bubbles extract substantial heat from the surrounding melt, resulting in localized undercooling[27]. This undercooling enhances nucleation, thereby increasing grain density and reducing grain size. As cavitation bubbles continue to grow and eventually collapse, they produce transient high-pressure pulses[28]. According to the Clausius-Clapeyron relation, the crystallization temperature of the alloy increases with pressure[29]. Thus, the pressure surge from bubble collapse elevates the melt's crystallization temperature, further enhancing undercooling and promoting the nucleation of α-Mg grains. Concurrently, the propagation of ultrasonic waves within the melt generates convective flow, forming a recirculating acoustic streaming pattern that intensifies turbulence. This flow promotes a more uniform distribution of solute elements and reduces temperature gradients across the melt[30]. As a result, the composition and temperature fields at the solid-liquid interface of α-Mg grains become more homogeneous, mitigating directional disparities in solute and thermal gradients. Consequently, grain growth rates become more isotropic, facilitating the development of a spherical growth morphology.

Fig.3 presents X-ray diffraction (XRD) patterns of the Mg-12Gd-0.5Zr alloy subjected to varying ultrasonic powers. The microstructure primarily comprises α-Mg and Mg_5Gd phases. According to the phase diagram calculations in Fig.1, the α-Zr

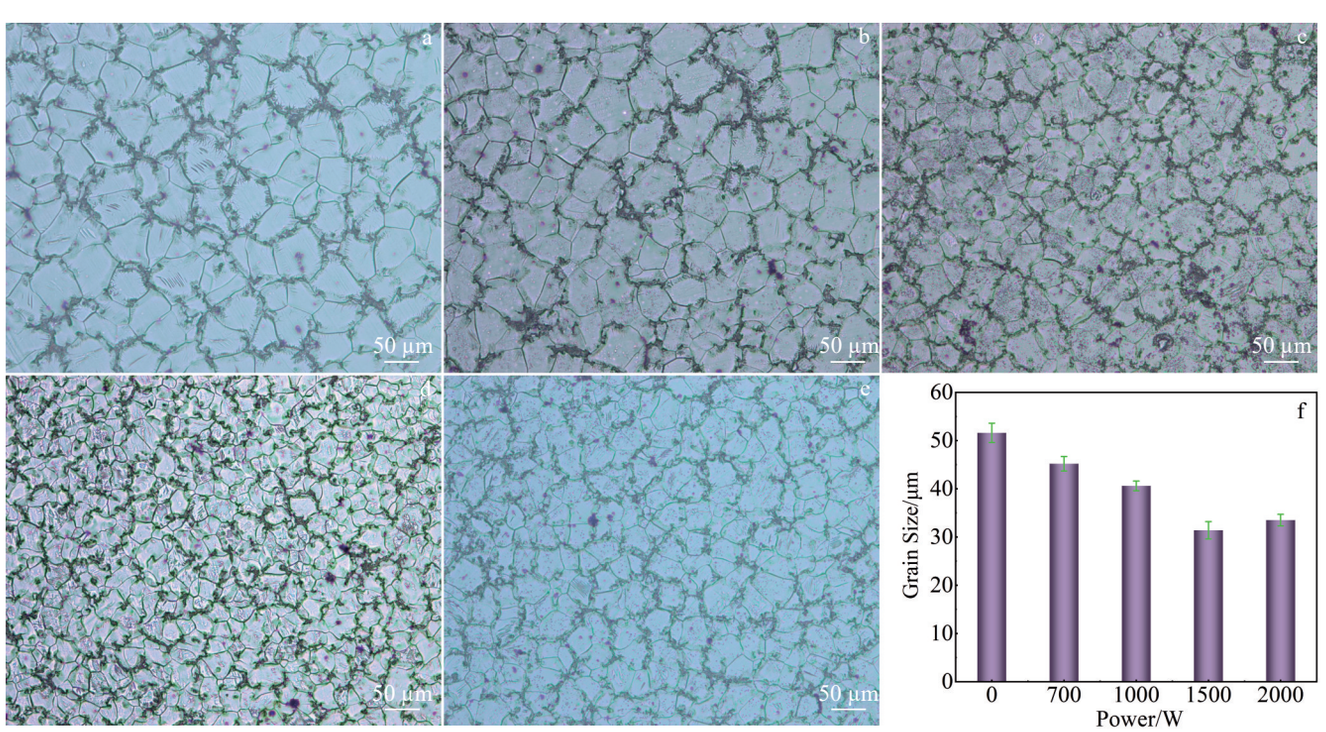

Fig.2 OM images of Mg-12Gd-0.5Zr alloys (a–e) and average size of the α-Mg phase (f) at varying ultrasonic powers: (a) 0 W, (b) 700 W, (c) 1000 W, (d) 1500 W, and (e) 2000 W

phase is expected to be present; however, it is not detected in XRD patterns in Fig. 3. This absence is likely due to the relatively low volume fraction of the α-Zr phase. Furthermore, the intensity of the Mg_5Gd diffraction peaks decreases significantly after ultrasonic treatment, indicating a reduced amount of this phase in the matrix. These results suggest that ultrasonic treatment facilitates the dissolution of the secondary phase into the α-Mg matrix.

Fig.4 presents low-magnification SEM morphologies of the as-cast Mg-12Gd-0.5Zr alloy at various ultrasonic powers. According to XRD patterns and phase-diagram analysis, the secondary phase at the grain boundaries is identified as the Mg_5Gd phase. In Fig. 4a, the Mg_5Gd phase in the untreated alloy appears as a coarse, semi-continuous network along the grain boundaries. As shown in Fig. 4b – 4c, this network morphology remains largely unchanged at ultrasonic powers of 700 and 1000 W, although the phase features become

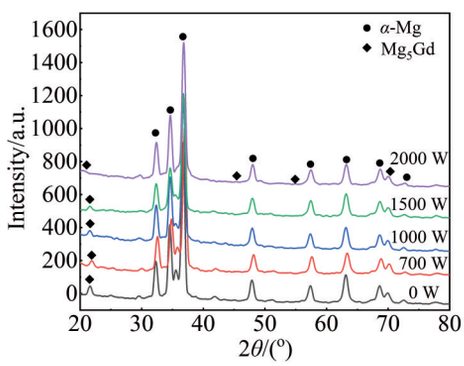

Fig.3 XRD patterns of the Mg-12Gd-0.5Zr alloys at varying ultrasonic powers

significantly refined. When the ultrasonic power is increased to 1500 and 2000 W, most of the Mg_5Gd phase transitions to a fine, fishbone-like morphology. This structural transformation enhances interfacial bonding with the matrix, thereby promoting dispersion strengthening. Fig. 4f shows the area fraction of the Mg_5Gd phase in the alloy at different ultrasonic powers. The area fraction initially decreases and then increases with increasing ultrasonic power, reaching its minimum at 1500 W. Specifically, the area fractions of the Mg_5Gd phase at 0, 700, 1000, 1500, and 2000 W are 5.93%, 5.86%, 5.75%, 4.29%, and 3.86%, respectively. These results indicate that ultrasonic treatment inhibits the precipitation of the Mg_5Gd phase, consistent with the XRD findings.

Fig. 5 presents high-magnification SEM images of the as-cast Mg-12Gd-0.5Zr alloy at varying ultrasonic power levels. The transformation of the Mg_5Gd phase from a network-like to a fishbone-like morphology under ultrasonic irradiation is more clearly observed, consistent with the findings in Fig. 4. To elucidate the correlation between the morphology of the Mg_5Gd phase and its composition, EDS analysis was performed on 10 individual Mg_5Gd phases obtained from alloys subjected to different ultrasonic powers. The statistical results for the variation in Gd content are shown in Fig. 5e. The data reveal that the fishbone-like Mg_5Gd phase has a lower Gd concentration than its network-shaped counterpart. Additionally, the Gd content in the Mg_5Gd phase initially decreases and then increases with increasing ultrasonic power, reaching a minimum at 1500 W. This trend suggests that ultrasonic treatment promotes the dissolution of Gd into the α-Mg matrix.

Following ultrasonic treatment, the secondary phase in the alloy is significantly refined and exhibits a more uniform

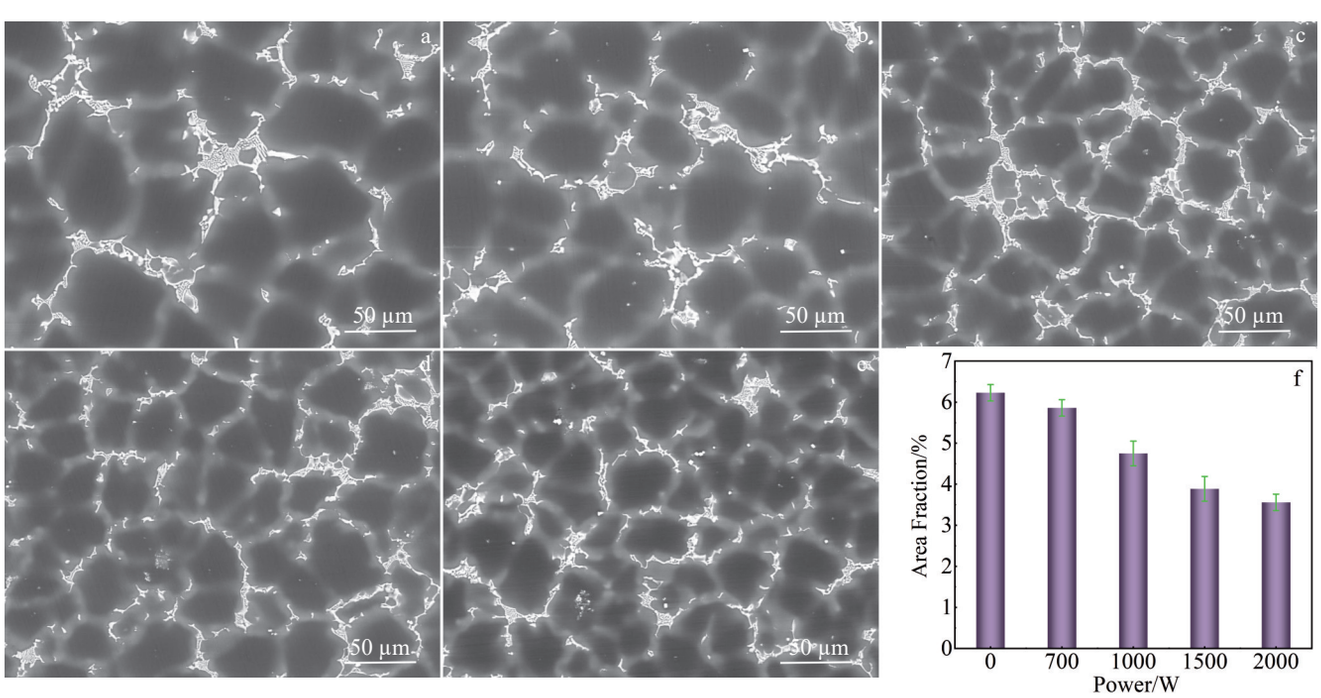

Fig.4 SEM images of Mg-12Gd-0.5Zr alloys (a–e) and area fraction of Mg_5Gd phase (f) at varying ultrasonic powers: (a) 0 W, (b) 700 W, (c) 1000 W, (d) 1500 W, and (e) 2000 W

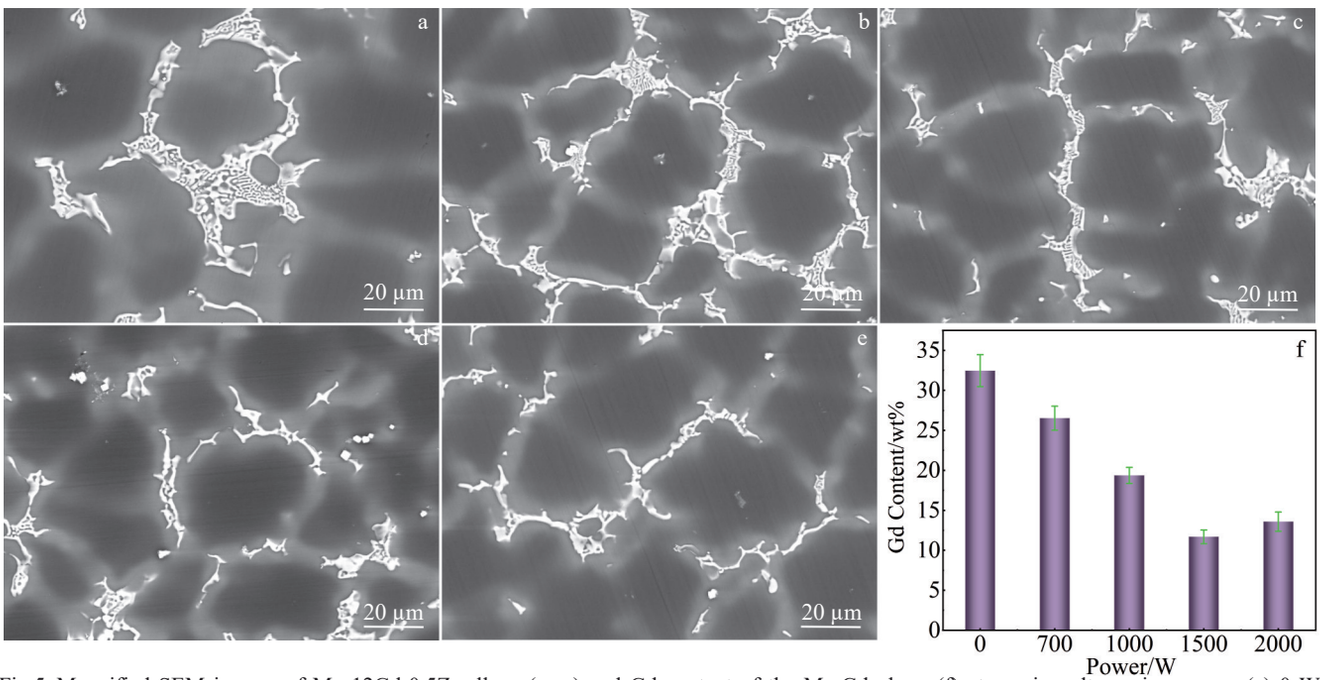

Fig.5 Magnified SEM images of Mg-12Gd-0.5Zr alloys (a–e) and Gd content of the Mg_5Gd phase (f) at varying ultrasonic powers: (a) 0 W, (b) 700 W, (c) 1000 W, (d) 1500 W, and (e) 2000 W

distribution. In contrast, during direct solidification without ultrasonic assistance, elemental segregation readily occurs. At the advancing solid-liquid interface, regions enriched in alloying elements promote the preferential nucleation and growth of the Mg_5Gd phase, resulting in the formation of coarse Mg_5Gd phases in these areas. Conversely, in regions with lower concentrations of alloying elements, the growth of the Mg_5Gd phase is inhibited, resulting in much smaller phase sizes. As a result, substantial size variations in the Mg_5Gd phase are observed throughout the alloy. The acoustic streaming effect induced by ultrasonic treatment effectively alleviates solute segregation. During ultrasonic processing, α-Mg grains are uniformly dispersed in the melt. As these grains grow, solute elements continuously accumulate at the progressing solid-liquid interfaces. Acoustic streaming facilitates the formation of more uniformly distributed α-Mg grains, thereby reducing intergranular spacing and mitigating compositional differences in solute enrichment at grain boundaries. Consequently, during subsequent cooling and forming, the Mg_5Gd phase forms under constrained solute concentration and spatial conditions, thereby suppressing its growth and yielding smaller Mg_5Gd phases. Moreover, ultrasonic treatment alters the chemical composition of the Mg_5Gd phase. Specifically, the Mg_5Gd content in the phase is reduced, indicating reduced participation of Gd atoms in the formation of the Mg_5Gd phase during solidification. This transformation primarily occurs because the collapse of cavitation bubbles promotes melt undercooling, thereby enhancing the solid solubility of Gd in the matrix. Additionally, the implosion of cavitation bubbles fragments secondary phases within the melt, reducing solidification time and further enhancing the dissolution of element Gd into the matrix.

3.3 Mechanical properties

Fig. 6 presents the tensile engineering stress-engineering strain curves and the variation in tensile properties of Mg-12Gd-0.5Zr alloys subjected to different ultrasonic powers, tested at 25 °C. Ultrasonic treatment at varying power levels significantly improves the ultimate tensile strength (UTS), yield strength (YS), and elongation of the as-cast Mg-12Gd-0.5Zr alloy to different extents. As ultrasonic power increases, both strength and elongation initially increase, and then decline. For the untreated alloy, the UTS, YS, and elongation at room temperature are 144.5 MPa, 86 MPa, and 1.56%, respectively. At 1500 W, the alloy exhibits peak performance, with UTS, YS, and elongation reaching 219.6 MPa, 148 MPa, and 3.27%, respectively. Further increasing the ultrasonic power to 2000 W results in a decline in both strength and elongation. The enhancement in strength is primarily attributed to microstructural refinement, including grain and second-phase particle refinement. Moreover, ultrasonic treatment reduces segregation of the secondary phase, as evidenced by the SEM images in Fig. 4, thereby contributing to improved elongation.

Comprehensive experimental investigations demonstrate that the enhancement of the mechanical properties of as-cast Mg-12Gd-0.5Zr alloy by ultrasonic treatment results from three synergistic mechanisms. Firstly, ultrasonic treatment induces substantial microstructural refinement; coarse dendritic structures are transformed to rounded equiaxed grains via acoustic streaming and cavitation. Refined grains increase strength and ductility via the Hall-Petch relationship. Secondly, ultrasonic vibration modifies the morphology of the secondary phase, converting the initially coarse, semi-

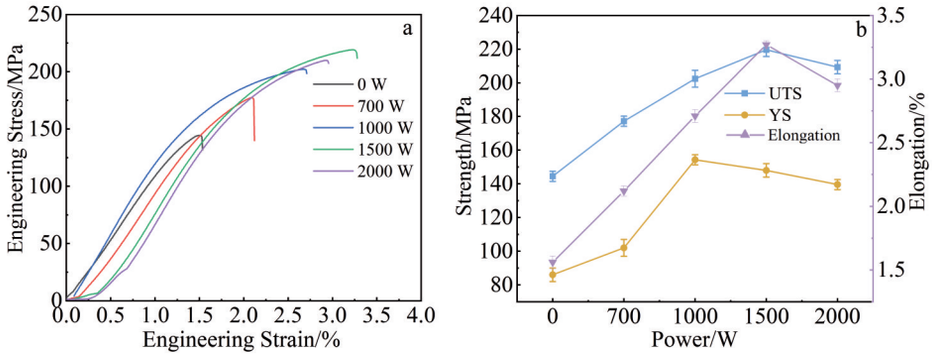

Fig.6 Tensile engineering stress-engineering strain curves (a) and changes in tensile properties (b) of Mg-12Gd-0.5Zr alloys

continuous network-like Mg_5Gd phase into a finely dispersed, fishbone-like structure with improved uniformity. These fine Mg_5Gd phases effectively impede dislocation motion through the Orowan strengthening mechanism. More importantly, the localized high-temperature and high-pressure conditions generated by cavitation significantly promote the dissolution of Gd atoms into the matrix. The resulting supersaturated solid solution induces severe lattice distortion, thereby facilitating solid solution strengthening. The combined effects of grain boundary strengthening, secondary-phase strengthening, and solid-solution strengthening constitute the primary mechanism underlying the improved mechanical performance. In addition, the refined secondary phases help suppress crack initiation by alleviating stress concentrations, further enhancing the alloy's plastic deformation capability.

The influence of ultrasonic treatment on the alloy's tensile behavior is further elucidated by examining its fracture morphology. As shown in Fig. 7, the tensile fracture surfaces comprise cleavage planes, cleavage steps, dimples, and river patterns. Arrow 1 indicates dimples, arrow 2 denotes cleavage planes, and circles highlight cleavage steps. In the absence of ultrasonic treatment, numerous cleavage planes and steps are observed, while dimples are sparse, indicating a typical brittle fracture. With increasing ultrasonic power to 700 and 1000 W, the presence of cleavage planes is significantly reduced, and dimple density increases. When the power is further raised to 1500 and 2000 W, cleavage planes become negligible, and densely distributed dimples dominate the fracture surfaces. This transformation is attributed to grain refinement and the concurrent refinement of Mg_5Gd phases under ultrasonic treatment. In the untreated alloy, cracks readily initiate at the interface between large, brittle Mg_5Gd phases and propagate rapidly through the interconnected network, resulting in a predominantly cleavage fracture with minimal energy absorption. After ultrasonic refinement, the well-dispersed, fine Mg_5Gd particles are less effective as crack initiation sites. Consequently, plastic deformation of the α -Mg matrix becomes the dominant process. The refined grains and dissolved Gd enhance the matrix's strength, requiring higher stress to activate dislocation movement. This leads to

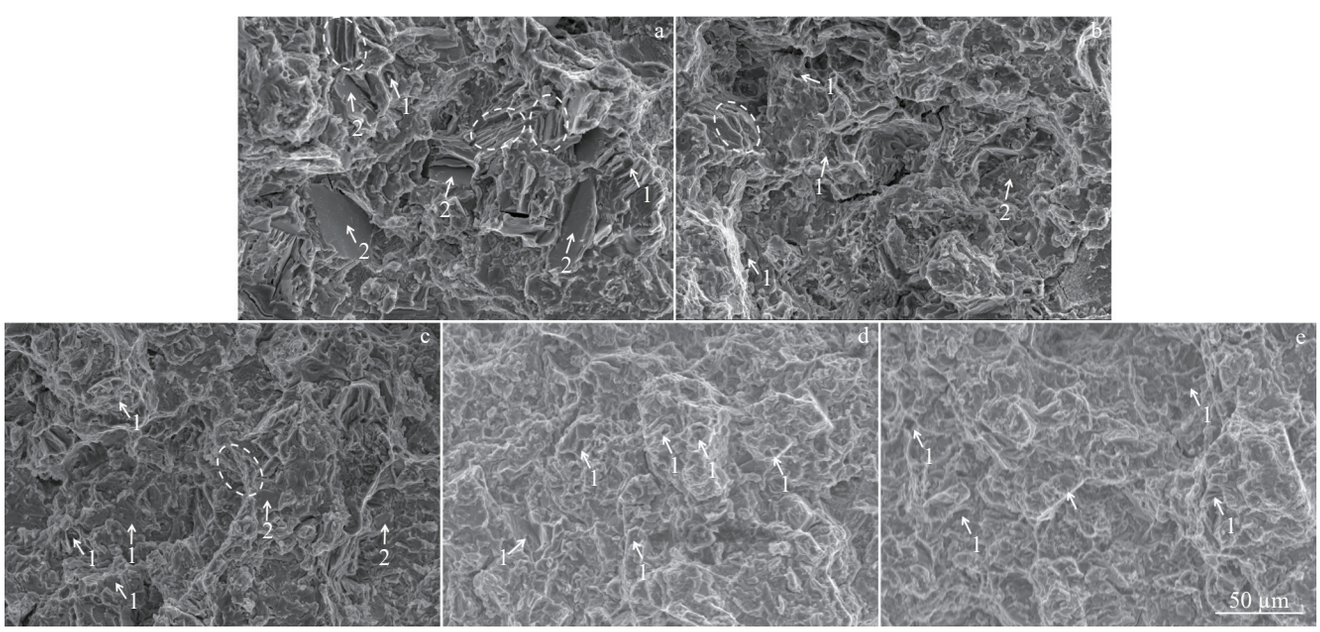

Fig.7 Tensile fracture morphologies of the as-cast Mg-12Gd-0.5Zr alloys at varying ultrasonic powers: (a) 0 W, (b) 700 W, (c) 1000 W, (d) 1500 W, and (e) 2000 W

significant energy dissipation through plastic deformation, as evidenced by numerous dimples on the fracture surface. The fine Mg_5Gd particles may also act as obstacles to dislocation glide, contributing to Orowan strengthening and further enhancing the energy required for fracture. Therefore, the refinement of Mg_5Gd phases improves elongation, with the alloy exhibiting a peak elongation of 3.27% after treatment at 1500 W.

4 Conclusions

1) Ultrasonic treatment can markedly refine the α-Mg grain size in the Mg-12Gd-0.5Zr alloy. With increasing ultrasonic power from 0 W to 2000 W, the α-Mg grain size initially decreases and then increases, reaching a minimum of 31.4 μm at 1500 W. This refinement is primarily attributed to cavitation and acoustic streaming effect induced by the ultrasonic field, which promotes heterogeneous nucleation.

2) The size of the secondary phase (Mg_5Gd) is substantially reduced, and its spatial distribution becomes more uniform after ultrasonic treatment. Moreover, the amount of secondary phases decreases, accompanied by a significant increase in dissolution of Gd atoms into the matrix. These effects arise from acoustic streaming, which suppresses the segregation of Gd at the solid-liquid interface.

3) The ultrasonic treatment leads to notable improvements in UTS, YS, and elongation at room temperature. These enhancements are primarily attributed to microstructural refinement and increased Gd solid solution in the matrix.

References

1 Li Y, Zhang A, Li C *et al. Journal of Materials Research and Technology*[J], 2023, 26: 2919

2 Zhao Lun, Sun Zhichao, Wang Chang *et al. Rare Metal Materials and Engineering*[J], 2025, 54(11): 2717 (in Chinese)

3 Jin Z, Zha M, Wang S *et al. Journal of Magnesium and Alloys*[J], 2022, 10: 1191

4 Yan Z, Yang Q, Ma R *et al. Materials Science and Engineering A*[J], 2022, 831: 142264

5 Wang C X, Min S Y, Liu J G *et al. Journal of Magnesium and Alloys*[J], 2023, 12(11): 4509

6 Zhao J, Jiang B, Yuan Y *et al. Materials Science and Engineering A*[J], 2020, 772: 138779

7 Stanford N, Atwell D, Barnett M R *et al. Acta Materialia*[J], 2010, 58: 6773

8 Li M, Huang Y, Liu Y *et al. Materials Science and Engineering A*[J], 2022, 832: 142479

9 Yu Z, Xu C, Meng J *et al. Journal of Alloys and Compounds*[J], 2017, 729: 627

10 Xu C, Nakata T, Qiao X G *et al. Scientific Reports*[J], 2017, 7: 43391

11 Zheng J, Chen Z, Yan Z M *et al. Materials Science and Engineering A*[J], 2021, 828: 142103

12 Nie J F, Gao X, Zhu S M *et al. Scripta Materialia*[J], 2005, 53: 1049

13 Zhen Rui, Sun Yangshan, Shen Xuewei *et al. Rare Metal Materials and Engineering*[J], 2018, 47(10): 2957 (in Chinese)

14 Yan Liangming, Liu Yuhao, Shi Ge *et al. Rare Metal Materials and Engineering*[J], 2018, 47(5): 1393 (in Chinese)

15 Rong W, Zhang Y, Wu Y J *et al. Materials Science and Engineering A*[J], 2019, 740: 262

16 Yan Z, Li X, Zheng J *et al. Journal of Magnesium and Alloys*[J], 2021, 9(3): 964

17 Gao D M, Li Z J, Han Q Y *et al. Materials Science and Engineering A*[J], 2009, 502: 2

18 Wang F, Eskin D, Mi J W *et al. Acta Materialia*[J], 2016, 116: 354

19 Hu Z, Li X, Yan H *et al. Journal of Alloys and Compounds*[J], 2016, 685: 58

20 Chen R R, Zheng D S, Guo J J *et al. Materials Science and Engineering A*[J], 2016, 653: 23

21 Dong X B, Guo Y C, Li J P *et al. Rare Metal Materials and Engineering*[J], 2022, 51(01): 11

22 Yu J C, Fang H Z, Hao J Q *et al. Journal of Alloys and Compounds*[J], 2024, 989: 174412

23 Liu X, Osawa Y, Takamori S *et al. Materials Science and Engineering A*[J], 2008, 487(1–2): 120

24 Tong X, You G Q, Wang Y C *et al. Materials Science and Engineering A*[J], 2018, 731: 44

25 Yang X, Wu S S, Lü S L *et al. Ultrasonics Sonochemistry*[J], 2018, 487: 472

26 Dong X B, Guo Y C, Li J P *et al. Advanced Engineering Materials*[J], 2020, 1901590: 1

27 Shen Y Z, Wang K, Li H N *et al. Materials Science and Engineering A*[J], 2024, 895: 146222

28 Pan M, Wang J X, Bai S *et al. Journal of Materials Research and Technology*[J], 2024, 30: 6064

29 Yin Z Y, Le Q C, Chen X R *et al. Journal of Materials Research and Technology*[J], 2022, 21: 1554

30 Jang H S, Lee G H, Jeon J B *et al. Journal of Materials Research and Technology*[J], 2022, 19: 2645

超声处理提高铸态 Mg-12Gd-0.5Zr 合金微观组织和力学性能

钟　浩[1,3]，董雄博[2]，杨　伟[1]，王雪怡[2]，马志军[1]，杨　忠[1]

（1. 西安工业大学 材料与化工学院，陕西 西安 710021）

（2. 陕西铁路工程职业技术学院，陕西 渭南 714000）

（3. 榆林学院，陕西 榆林 719000）

摘　要：探讨了超声处理对铸造Mg-12Gd-0.5Zr合金微观组织和拉伸性能的影响。结果表明，超声处理可显著细化α-Mg晶粒组织，在1500 W功率下晶粒细化效果最佳。这种晶粒细化效果归因于超声场空化效应与声流效应的协同作用，从而促进异质形核。此外，超声处理在改善Mg_5Gd第二相空间分布均匀性的基础上，有效控制了其析出尺寸并减少了析出数量。超声处理后，合金中Gd元素在α-Mg基体中的固溶度显著提高，这主要得益于声流效应对元素偏析的抑制作用。相应地，经过超声处理的合金在室温条件下表现出更优异的综合力学性能，其抗拉强度、屈服强度和伸长率均得到同步提升，这些性能改善主要归因于显微组织的细化以及基体中Gd固溶度的提高。

关键词：镁合金；超声处理；晶粒细化；拉伸性能

作者简介：钟　浩，男，1986年生，硕士，西安工业大学材料与化工学院，陕西 西安 710021，电话：029-86173324，E-mail：zhonghao_2025@163.com